Clays and Clay Minerals, Vol. 47, No. 1, 54–63, 1999.

APPLYING X-RAY GEOTHERMOMETER DIFFRACTION TO A CHLORITE

STEFANO BATTAGLIA

International Institute for Geothermal Research C.N.R., 2 Piazza Solferino, 56126 Pisa, Italy

Abstract—A new method is proposed for applying the chlorite geothermometer using X-ray diffraction (XRD) data. A linear correlation has been found between the (001) basal spacing of chlorite and its "crystallization" temperature. The basal spacing values were corrected for an increase of Al(IV) with Fe enrichment (Fe/Fe + Mg), when the Fe(II) value of chlorite is > 2.6 in the formula unit. The regression coefficient of the best fit is r = 0.95. Only 2 Bragg lines need to be measured for application of the proposed technique: the (001) and (060) X-ray spacing. The proposed method is applied to 19 chlorite samples from 4 different geothermal fields. The temperatures of chlorite formation obtained with the present method and those calculated by the expressions formulated by Cathelineau (1988) and Kranidiotis and MacLean (1987) are presented. The method's validity was also tested on geothermal chlorites from the literature, and the results show good agreement with previous experimental trials.

Key Words—Chlorite Geothermometer, X-Ray Diffraction.

INTRODUCTION

Chlorite minerals are a principal component of a great variety of rocks, including sedimentary, low-grade metamorphic and hydrothermally altered rocks. By virtue of the wide variability in its composition, chlorite can act as a record of the chemical and physical variations occurring during its formation. Thus, by characterizing the chemical transformation of chlorite we can study the genesis, metamorphism and hydrothermal alteration of ore deposits. A number of works have noted a systematic decrease in the Si content (IV) and increase in Al(IV) of chlorites with increasing depth in diagenetic and geothermal systems (McDowell and Elders 1980; Jahren and Aagaard 1989). In particular, Cathelineau and Nieva (1985) and Cathelineau (1988) have found that such changes in makeup result from a progressive increase in the temperature of chlorite formation, with a positive correlation between Al(IV) content and temperature.

Chemical analyses of chlorites of varying composition and origin have also shown that, together with the increase in Al(IV) in tetrahedral sites, there is an increase in divalent cations, especially Fe and Mg. Consequently, several authors have suggested that a correction should be applied to the increment in Al(IV) with Fe/(Fe + Mg) (Kranidiotis and MacLean 1987). Such methods would require recourse to systematic analysis of the clay minerals performed by means of an expensive and time-consuming process using automatic electron microprobe equipment.

Another important find is that the transition of smectite into chlorite is one of the most important processes in low-grade metamorphism of mafic rocks and active geothermal systems, where chlorite minerals are frequently present (Helmold and Van de Kamp 1984; Inoue et al. 1984; Alt et al. 1986; Laird 1988; Reynolds 1988). By using high-resolution electron microscopy, some researchers (Roberson 1989; Shau et al. 1990) have shown that in the presence of this transition, mixtures of 2, or even 3 phases (smectite, chlorite and corrensite) can develop. These phases are formed as thin crystallites (Bettison-Varga and MacKinnon 1989; Shau et al. 1990) on a scale of hundreds of angstroms. In such situations the problem of chlorite purity is critical, and the resolution of an electron microprobe, the most commonly used analytical instrument, does not allow for direct determination of the purity of the chlorite under observation (Schiffman and Fridleifsson 1991). Only by recalculating the structural formula of phyllosilicate composition, using the method proposed by Bettison and Schiffman (1988), is it possible to achieve a correct estimation of the chlorite percentage present in the sample.

Given the above limitations and the fact that any study of clay minerals almost inevitably requires preliminary XRD tests, this paper proposes an analytical relation observable between the formation temperature of chlorite and its basal spacing, as estimated by the position of the (001) Bragg line. When the Fe value in the chlorite structural formula is >2.6, this basal spacing is then corrected for Fe and Mg occupancy in the chlorites under exam. In order to test the validity of the proposed equation, we analyzed samples originating from various geothermal fields. The data required to obtain the temperature values through the proposed relation can be provided by an XRD apparatus alone. The temperature values thus obtained were then compared to those yielded by the relation formulated by Cathelineau (1988) and Kranidiotis and MacLean (1987). In order to test the applicability of the method on a wider statistical basis, we also examined data from the literature on chlorites of geothermal origin.

THEORY

For trioctahedral chlorites, increasing the substitution of Al for Si in the tetrahedral sites decreases the thickness of the layer. The basal spacing depends on the dimensions of the talc-brucite layers. Thus, X-ray basal spacing methods can be utilized to estimate the Al content in the tetrahedral sites (Bailey 1972). More specifically, this spacing varies with the amount of Al(IV), according to the equation:

$$d^{M}_{001} = 14.5\ \text{Å} - 0.31\ x \qquad [1]$$

where the variable x = Al(IV) for 4.0 tetrahedral positions, and d^{M}_{001} is the measured value of the (001) diffraction line (Nemecz 1981). Other authors have proposed similar equations in which the constants may assume different values for the Fe(II) and Fe(III) chlorite content, (see Kepezhinskas 1965). The occupancy in the octahedral cation sites can be estimated for trioctahedral chlorites by measuring the (060) spacing (Von Engelhardt 1942; Shirozu 1958; Brindley 1961; Kepezhinskas 1965; and Bailey 1972) and using, for example, the equation from Shirozu (1958):

$$b = 9.21\ \text{Å} + 0.037\ y \qquad [2]$$

where y = Fe(II) is the number of ferrous ions in the octahedral positions. This led to a search for a linear relation between the chlorite-formation temperature and the corresponding value of its basal spacing, corrected in order to account for the Fe content d^{c}_{001}. The d^{c}_{001} value is related to the measured spacing d^{M}_{001} by a straight line that can be expressed as:

$$d^{c}_{001} = 14.5\ \text{Å} - 0.31\ x' \qquad [3]$$

where x' = Al(IV) + ((Fe/Fe + Mg)K), and K is an experimentally determined constant. The K constant was assigned the value of 0.8, which corresponds to the slope of the regression line of Al(IV) plotted against Fe/(Fe + Mg). Indeed, in the examined chlorites, there is an appreciable increase in Al(IV) content with iron enrichment (Fe/Fe + Mg). The resulting slope is very similar to the value reported by Kranidiotis et al. (1987) using microprobe data. In particular, if the chlorite formula is taken to be:

$$(Mg_{6-x-y}Fe^{II}_{y}Al_{x})(Si_{4-x}Al_{x})O_{10}(OH)_{8} \qquad [4]$$

by substituting in Equation [3] the values of Fe and Mg obtained from Equation [2] and the chlorite formula [4], respectively, and evaluating the Al(IV) value from Equation [1], we obtain the relationship:

$$d^{c}_{001} = d^{M}_{001} - (0.077y/(d^{M}_{001} - 12.64)) \qquad [5]$$

GEOLOGICAL SETTING

The geological settings in the active geothermal fields from which the samples were collected, are as follows:

1) Aluto-Langano (Ethiopia) is a high-temperature, water-dominated geothermal system hosted in alkaline basalt to rhyolite lavas and pyroclastics within the Main Ethiopian Rift. The geology of the area has been described in detail by Lloyd (1977) and Di Paola (1972). The oldest outcropping rocks are found on the main eastern rift escarpment and consist mainly of coarsely porphyritic, strongly welded crystal ignimbrite flows, with minor rhyolite and basalt intercalations, commonly known as the "Tertiary ignimbrite" unit. Its thickness is about 700 m. This unit is overlain by a fissural basaltic unit (called "Bofa basalt") with a thickness of about 800–1000 m. In local outcroppings the basalt is made up of an intersertal groundmass and phenocrystals of plagioclase, olivine, augite and oxides. The "Bofa basalt" units are covered by lacustrine sediments (Pleistocene-Holocene) that are predominantly fine-grained vitric tuffs, sandstones and pumiceous rhyolitic gravels. Their maximum thickness is 400 m. The Quaternary Aluto volcanic products have radiometric ages ranging from 155,000 ± 8000 (K/Ar method, Hulo-Seyno ignimbrite) to 2000 y (^{14}C method, Electroconsult 1986). A minimum age of 140,000 y has been suggested for the Aluto-Langano geothermal system through modeling of time-variant heat-transfer patterns (Hochstein et al. 1983). The origin of the geothermal system could therefore be contemporaneous with the earliest eruptions of ash flow tuffs, lithic breccias and pumice flow at Aluto. Eight deep exploratory wells (called "LA1-8 wells") have been drilled at Aluto. We examined samples from wells LA3 and LA6, drilled in a high-temperature part of the system (upflow zone) and from LA4 and LA7 where outflow zones were encountered. The alteration mineral assemblages found in the geothermal field of Aluto-Langano indicate a complex evolution of water-rock interaction processes. The zone of upflow is characterized by the presence of a propylitic alteration (epidote, calcite, quartz and chlorite, as major phases) coexisting with calcite and clay minerals. The zone of lateral outflow is characterized by the occurrence of an argillic (calcite + clay minerals), marked by the presence of smectite, illite–smectite mixed layers, illite and minor amounts of mixed chlorite–smectite layers, vermiculite, chloritic-intergrade and kaolinite (Gianelli and Teklemariam 1993; Teklemariam et al. 1993; Teklemariam et al. 1996).

2) Tendaho is an active geothermal field in the Afar region (Ethiopia). The area of Tendaho corresponds to a 50-km-wide rift with a NW-SE trending structure, which can be considered the southern extension on land of the Red Sea structure joining the Ethiopian rift. The structural geology of the area has been reviewed by Abbate et al. (1995). The lacustrine and alluvial deposits, basalts of the Afar Series with associated rhyolites, are the main rocks in this system. Four wells have been drilled (TD1-4) in the area. For the purposes

https://doi.org/10.1346/CCMN.1999.0470106 Published online by Cambridge University Press

of the present study, core samples from wells TD1, TD2 and TD3 were examined. Hydrothermal alteration is widely present along sections of the drilled wells and testifies to important processes of water-rock interaction. Chemical-petrografic data on core samples (altered basalts) show that calcite, wairakite, laumontite, garnet, epidote, pyroxene, quartz and prehnite are common non-clay hydrothermal minerals. The clay minerals present are chlorite, vermiculite, smectite and chlorite–smectite interlayers. Petrographic study shows a) evidence of an early stage of calcite, zeolite and quartz crystallization, while calcite underwent different stages of dissolution/precipitation, and b) that epidote, garnet, prehnite, pyroxene and amphibole crystallization occurred after wairakite or laumontite (Aquater 1994a, 1994b). The hydrothermal activity is indicated by silica deposition within NW to NNW subvertical fractures cross-cutting the rift sediments. The veins are made up of microcrystalline quartz with minor calcite, stilbite and smectite. Absolute dating using the $^{230}Th/^{234}U$ method was performed on a quartz–calcite vein and yielded an age of 12,000 ± 5000 y (Abbate et al. 1995).

3) The island of St. Lucia (Lesser Antilles) where 2 wells, SL-1 and SL-2, have been drilled in the Qualibou caldera (Soufrière), contains a high-temperature geothermal system. The magma body associated with the formation of the caldera must be a major source of heat contributing to the Sulphur Springs geothermal area today. The K/Ar and ^{14}C dates of this event range from 32,000 to at least 39,000 y (Westercamp and Tomblin 1980; Wohletz et al. 1986). The island of Saint Lucia belongs to the Windward Islands in the Lesser Antilles, and is located between Martinique and St. Vincent. The island is made up almost exclusively of volcanic products, ranging from basalts to andesites and dacites, coming from various centers scattered over a number of sites. The Soufrière area exhibits surface thermal manifestations (Aspinall et al. 1976; Wohletz et al. 1986) in the form of boiling acid-sulphate springs and fumaroles. The hydrothermal alteration found in both the productive SL-2 well and the nonproductive SL-1 is similar to that occurring in many other geothermal systems in which the geothermal fluid reacts with andesitic and dacitic rocks (Steiner 1977). The mineral distribution with depth resembles the argillic, phyllitic and propilitic alterations of many porphyry copper deposits (Rose and Burt 1979), with a) an inner, high-temperature potassic zone characterized by the occurrence of dravitic tourmaline, quartz and biotite, b) an outer propylitic alteration zone that is partly superimposed on c) a potassic alteration zone (Battaglia et al. 1991). Four mineral zones can be distinguished in the SL-2 well from ground level to bottom-hole: i) kaolinite zone, ii) mixed illite and smectite layer zone, iii) illite zone and iv) epidote–actinolite zone. Chlorite is present from zone ii) to the bottom of the well. In the SL-1 well the following hydrothermal alteration zoning was found: a) a scarcely altered zone up to about 900 m, b) a calcite–clay minerals zone and c) a chlorite–albite–calcite-epidote zone.

4) The Monteverdi zone is sited on the western border of the Larderello geothermal field (Tuscany, Italy). From a geological point of view, this area is considered to be a structural high of the metamorphic substratum. Because of tectonic denudation of the carbonatic-evaporitic sequence, which usually constitutes the shallow geothermal reservoir in the Larderello field (Baldi et al. 1995), the cap-rock of Neogenic and Flysch units lies directly on the metamorphic formations. Among the various wells that have been drilled in this zone, we have considered wells MV-2 and MV-5. The mineralogy of the sample consists of chlorite, muscovite and quartz, with minor amounts of titanite, epidote and pyrite, for the core originating from the MV-2 well, while the core composition from MV-5 consists of quartz, white mica and hematite with a cement of calcite, chlorite, dolomite and minor amounts of anhydrite, albite and apatite (Gianelli and Bertini 1993). Baldi et al. (1995) state that "The hydrothermal mineral distribution with depth shows that the equilibrium temperature of the main minerals is in conformity with the current temperatures (calcite, quartz, chlorite, etc. up to 250 °C and epidote, K-feldspar, etc. over 250 °C). This, together with the dating of 60,000–10,000 y, obtained by $^{230}Th/^{234}U$ method on some secondary mineralizations, would indicate that Monteverdi hydrothermal system is very recent."

For further information regarding the geological setting, hydrothermal mineral zonations and thermal structure of these geothermal fields, the reader is referred to the papers cited above.

MATERIALS

We investigated 19 samples obtained as cores from drill holes located in the above-described geothermal systems. Core slides of 2–4 cm were first broken into pieces of less than 0.5 cm in diameter and then ground in a micronizing mill to obtain powdered samples.

The coarsely crushed samples were then disaggregated using ultrasonic vibration. Sedimentation in water was carried out in order to effect separation of the phyllosilicates from other mineralogical phases. The 2-μm fraction was used to prepare oriented and random mounts for XRD. Oriented specimens were obtained by removing the 2-μm fraction with a pipette and placing the suspensions on a glass slide. Duplicate oriented tiles were examined for each sample: one was air dried overnight and then analyzed; the other was saturated with 1 *M* KCl, dried and analyzed to test for the presence of vermiculite. The unoriented clay fractions were prepared by packing the dried material in hollow aluminum holders. In addition, thin polished

sections were prepared from drill cores for chemical analysis of authigenic chlorites through energy-dispersive microprobe analysis (EDS), for the samples coming from St. Lucia geothermal area, and by means of an automated electron microprobe in the wavelength dispersive mode (WDS) for all other chlorite samples examined.

ANALYTICAL METHODS

XRD analyses on basally and randomly oriented samples were performed with a Philips diffractometer using Cu-filtered Ni radiation at 40 kV and 25 mA, under the following analytical conditions: basally oriented slides were scanned between 2 and 33 °2θ, while the randomly oriented samples were scanned between 58 and 65 °2θ with a data resolution of 0.05 °2θ. A step size of 0.005 °2θ and a scan speed °2θ/s of 0.005 were employed for both sample series. Chemical analyses of chlorite minerals were conducted by means of 1) an automatic electron microprobe (Jeol-FXA-8600) using the following parameters: acceleration voltage 15 kV, excitation current 10 nA and count time 15 s; the correction program developed by Bence and Albee (1968) was applied; 2) an X-ray energy-dispersive system (EDAX PV9900) applied to a Philips 515 scanning electron microscope operating at the following analytical conditions: acceleration voltage 15 kV, excitation current 20 mA, beam spot size 0.2 μm, counting time 50 s. Raw data were corrected by applying the ZAF correction program proposed by Mickledust et al. (1978), then processed through a PV SUPQ program, which yielded mineral compositions recalculated to a 100% content on an anhydrous basis.

RESULTS AND DISCUSSION

Table 1 shows the results of chlorite microprobe analyses; the structural formulas were calculated on the basis of 14 oxygen molecules. The analyses presented in Table 1 are based on the average values from several points (at least 5 within a selected chlorite grain). Representative errors (standard deviations, σ) for the major oxides are presented in parentheses in column 1 of Table 1. As a double check of chlorite purity, the recalculated cation proportions of the analyses reported in Table 1 were used to determine the content of chlorite in each analysis, using the method proposed by Bettison and Schiffman (1988). These data are included in Table 1 and confirm what X-ray tests revealed: all the examined chlorites are characterized by a basal reflection with $d_{001} \cong 14.2$ Å, which is unaffected (or only very slightly influenced) by either ethylene glycolation or heating, so that the presence of interlayers can be excluded. The applicability of the chlorite geothermometer to all the selected samples is also confirmed because, for a chlorite percentage, x, (the proportion of chlorite to swelling component) ranging from 0.55 to 1.0 (pure chlorite), there is a good correlation between x and the temperature of formation (Bevins et al. 1991). Although the technique used for the chlorite analysis does not distinguish between divalent and trivalent Fe, a large number of chlorite analyses reported in the literature have determined that trivalent Fe constitutes less than 5% of the total (Deer et al. 1962; Foster 1962; Shirozu 1978). Therefore, in this study, all Fe measured is considered to be divalent.

In the chlorite analyses reported in Table 1, the largest proportional variation occurs for FeO (14.30–41.12 wt%) and MgO (1.43–23.81 wt%). Smaller variations are observed for SiO_2 (22.77–32.45 wt%) and Al_2O_3 (11.88–23.00 wt%). The Si content and Fe/(Fe + Mg) ratios have been used on a diagram designed by Hey (1954), see Figure 1, in chlorite classification. This figure reveals the wide range of chlorite solid solution in Fe-Mg and a more limited substitution of Al for Si, with a compositional variability ranging from clinochlore, ripidolite, pycnochlorite, diabantite to brunsvigite, thus illustrating the wide representativity of the chlorite samples examined. The Fe/(Fe + Mg) ratio in Figure 1 varies from 0.25 to 0.94, whereas in Cathelineau and Nieva (1985) the ratio is restricted to the 0.27–0.38 range. The relationship between chlorite composition and parent rock composition has been well illustrated by Laird's diagram (1988): in Figure 2 the atomic ratios Al/(Al + Fe + Mg) are plotted versus Mg/(Mg + Fe) for the studied chlorites. The figure shows that the Mg/(Mg + Fe) ratios of all the chlorites range from 0.06 to 0.75 and the Al/(Al + Fe + Mg) ratios from 0.23 to 0.39, with most samples lower than 0.35, which eliminates the presence of pelitic samples. All the samples examined are mafic or Fe-rich mafic rocks. Table 2 presents the results of direct temperature measurements (T_M) in drill-holes of the geothermal fields studied, using Kuster equipment (Model KT element within a tolerance of 1–2 °C in the temperature range 30–370 °C). The data given in this table are the actual temperatures in the fields. As these geothermal fields are very young (see the chronology of these areas reported in the geological setting) and the mineral assemblages are generally in agreement with the thermal conditions of the fields, indicating that large-scale heating or cooling did not occur after activation of the geothermal fields, the T_M values can be considered as estimates of the crystallization temperature of chlorites (see Cathelineau and Nieva 1985; Cathelineau 1988; De Caritat et al. 1993). Table 2 also reports the temperature of chlorite crystallization as calculated by the equations proposed by Cathelineau (1988) (T_c) and Kranidiotis and MacLean (1987) (T_{KM}), using the data reported in Table 1. The X-ray spacings of the Bragg (001) d^M_{001} and (060) d^M_{060} lines were measured, and their values are included in Table 2. As the accuracy of the spacing determinations was of critical importance, PC-APD (PW1877) Analytical

https://doi.org/10.1346/CCMN.1999.0470106 Published online by Cambridge University Press

Table 1. Mean electron microprobe chemical analysis of the examined chlorites. Estimate of the proportion of chlorite fraction relative to swelling component (see text). Chlorite sample name = name of well + sampling depth (m).

Well Dp. (m) No. of spot analyses	Chlorite samples											
	LA6† 670 6	LA6† 1508 7	LA4† 1000 8	LA3 1450 6	LA7† 550 6	LA7† 798 7	LA7† 1790 6	TD 1 1588 8	TD 1 2010 7	TD 2 800 6	TD 2 1200 6	TD 2 1500 8
SiO_2	29.77 (0.49)	27.19	27.64	32.34	22.77	24.64	29.69	31.39	29.84	29.21	28.84	29.49
TiO_2	0.09	0.01	0.04	0.09	0.05	0.00	0.24	0.02	0.05	0.02	0.02	0.04
Al_2O_3	18.04 (0.41)	18.61	18.15	11.88	15.50	17.23	14.39	15.18	15.57	16.27	17.65	16.35
FeO	25.53 (0.96)	23.74	31.78	25.10	41.12	38.52	18.53	22.58	27.40	23.20	22.02	34.08
MnO	0.27	0.47	0.95	0.23	1.72	2.35	0.44	0.25	0.29	0.24	0.38	0.59
MgO	15.13 (0.51)	16.54	9.36	17.81	1.43	1.58	20.08	17.57	15.21	15.92	18.60	9.45
CaO	0.21	0.09	0.18	0.25	0.25	0.29	0.52	0.28	0.36	0.36	0.14	0.30
Na_2O	0.14	0.07	0.04	0.21	0.07	0.18	0.17	0.12	0.13	0.08	0.04	0.19
K_2O	0.11	0.02	0.01	0.06	0.02	0.16	0.11	0.08	0.02	0.02	0.03	0.09
Tot.	89.29	86.74	88.15	87.97	82.92	84.95	84.16	87.47	88.87	85.32	87.72	90.58
Structural formulas based on 14 oxygens												
Si	3.06	2.88	2.99	3.36	2.87	2.95	3.16	3.24	3.12	3.12	3.00	3.14
Al^{IV}	0.94	1.12	1.01	0.64	1.13	1.05	0.84	0.76	0.88	0.88	1.00	0.86
Sum T	4.00	4.00	4.00	4.00	4.00	4.00	4.00	4.00	4.00	4.00	4.00	4.00
Al^{IV}	1.25	1.20	1.31	0.82	1.16	1.38	0.96	1.09	1.05	1.17	1.14	1.19
Fe	2.20	2.10	2.87	2.24	4.32	3.86	1.65	1.95	2.40	2.07	1.85	3.03
Mn	0.02	0.04	0.09	0.02	0.19	0.24	0.04	0.02	0.03	0.02	0.07	0.05
Mg	2.32	2.61	1.51	2.76	0.27	0.28	3.18	2.71	2.38	2.54	2.86	1.50
Ti	0.01	0.00	0.00	0.01	0.00	0.00	0.02	0.00	0.00	0.00	0.00	0.00
Sum M	5.80	5.95	5.78	5.86	5.94	5.76	5.84	5.77	5.86	5.80	5.92	5.77
Ca	0.02	0.01	0.02	0.03	0.04	0.03	0.06	0.03	0.04	0.04	0.01	0.03
Na	0.03	0.02	0.01	0.03	0.02	0.04	0.04	0.02	0.03	0.02	0.00	0.04
K	0.01	0.00	0.08	0.01	0.00	0.03	0.01	0.01	0.00	0.00	0.00	0.01
Ca+Na+K	0.06	0.03	0.11	0.07	0.06	0.10	0.11	0.06	0.07	0.06	0.01	0.08
Estimate of the proportion of chlorite relative to swelling component: 1 = chlorite and 0 = saponite z = Al in tetrahedral sites; y = Al in octahedral sites												
$z > y$	0.80	0.95	0.76	0.84	0.98	0.76	0.85	0.76	0.84	0.81	0.91	0.76
$z < y$	0.80	0.95	0.86	0.93	0.98	0.82	0.94	0.83	0.92	0.87	0.91	0.83

† Literature data from Teklemariam et al. (1996).
‡ Chemical analyses done by EDS (see text).

Powder Diffraction software was employed. For basal reflection, this program was used in conjunction with measurements of higher order (001) reflections, and the spacing values of the (001) lines reported in Table 2 were the means of all the basal reflections that could be measured. The correlation line obtained by a least-squares fit method, between d^{M}_{001} and T_M, shows a regression coefficient of 0.77. The relative plot is reported in Figure 3, where the studied chlorites have been labeled from 1 to 19, as reported in Table 2. Samples 5, 6, 12 and 18, showing large negative scattering from the regression line, have a high Fe content (Fe > 3.0, see Table 1, or Fe > 2.6 with X-ray data, see Table 2). Such lower d^{M}_{001} basal spacings, as compared to samples having comparable Al(IV) values, conform to the conclusions reached by Bailey (1972) and can be attributed to the large Fe content. By adding 0.1 Å to the measured (001) spacings of samples 5, 6, 12 and 18, as suggested by the above-mentioned author, the regression coefficient of the line correlating d^{M}_{001} to T_M is about 0.93.

A better correlation was found between the d^{c}_{001} values and the directly measured temperatures T_M. Using Equation [2], it is possible to determine the values of y = Fe(II) reported in Table 2. Then, by substituting these in the proposed Equation [5], we obtain the d^{c}_{001} values also listed in Table 2. For samples 5, 6, 12 and 18, no correction was employed for the Fe/(Fe + Mg) ratio enrichment with increased Al(IV). For these samples, the measured d^{M}_{001} values were inserted in the plot of d^{c}_{001} vs. temperature (Figure 4). The coefficient of the regression line is r = 0.95, with intercept = 14.379 and slope = −0.001. Using this regression line, the formation temperatures of chlorites were recalculated, and the values (T_{RX}) are reported in Table 2. In Figure 4 (T_M vs. d^{c}_{001} for the samples with Fe content < 2.6, and T_M vs. d^{M}_{001} for the samples with Fe content > 2.6), some of the more scattered samples come from drill-holes that have undergone cooling processes, such as TD3-1440 and LA4-1000 samples, or heating processes, such as for LA6-1508 sample. In fact, sample TD3-1440 comes from a well that seems to be

Table 1. Extended.

Chlorite samples						
TD 3 650 6	TD 3 1440 5	SL1‡ 1550 6	SL1‡ 1830 6	SL2‡ 1330 7	MV2 1870 8	MV5 1100 5
29.54	27.90	32.45	29.72	30.90	24.13	28.89
0.00	0.00	0.01	0.15	0.14	0.07	0.00
15.10	17.16	20.61	21.61	23.00	22.29	17.91
27.68	29.51	28.84	34.81	33.51	36.15	14.30
0.37	0.59	0.88	0.70	0.56	0.74	0.38
13.98	12.43	16.71	12.64	11.21	6.07	23.81
0.30	0.43	0.32	0.23	0.09	0.03	0.05
0.04	0.00	0.17	0.14	0.20	0.00	0.00
0.03	0.00	0.00	0.00	0.39	0.02	0.01
87.04	88.02	100	100	100	89.50	85.35
3.17	2.99	2.99	2.84	2.91	2.65	2.94
0.83	1.01	1.01	1.16	1.09	1.35	1.06
4.00	4.00	4.00	4.00	4.00	4.00	4.00
1.08	1.17	1.24	1.27	1.47	1.53	1.09
2.49	2.65	2.23	2.77	2.64	3.31	1.22
0.03	0.06	0.07	0.05	0.04	0.07	0.10
2.23	1.99	2.30	1.80	1.58	0.99	3.62
0.00	0.00	0.00	0.01	0.01	0.00	0.00
5.83	5.87	5.84	5.90	5.74	5.90	6.03
0.07	0.05	0.03	0.03	0.01	0.00	0.00
0.01	0.00	0.03	0.03	0.04	0.00	0.00
0.01	0.00	0.00	0.00	0.04	0.00	0.00
0.09	0.05	0.06	0.06	0.09	0.00	0.00
0.82	0.85	0.83	0.90	0.75	0.90	1.00
0.88	0.93	0.88	0.93	0.78	0.90	1.00

representative of a cooled system, for which a reasonable estimate of the temperature decrease would be at least 30–40 °C (Abbate et al. 1995), while sample LA4-1000 is located in an outflow zone that also underwent a significant cooling process (Teklemariam et al. 1996). On the other hand, the physical-chemical conditions and hydrothermal mineral assemblage of sample LA6-1508 indicate the occurrence of a heating process (Teklemariam et al. 1996). In other samples such as LA6-670, LA7-550 or LA7-1790, which come from hydrothermal systems that were subjected to similar heating or cooling processes, this scattering is less relevant.

In order to provide a thorough statistical assessment of the method's validity, it was applied to other data on geothermal chlorites drawn from the literature. Because of the absence in the literature of XRD data (001 and 060 X-ray spacing) on geothermal systems for chlorite crystallization temperatures, the chlorite chemical analyses from the geothermal system of Los Azufres (Mexico) and the Salton Sea (Gulf of California), consisting of 22 samples reported by Cathelineau (1988), were transformed using the relationship proposed by Rausell-Colom et al. (1991) and reformulated by Nieto (1997):

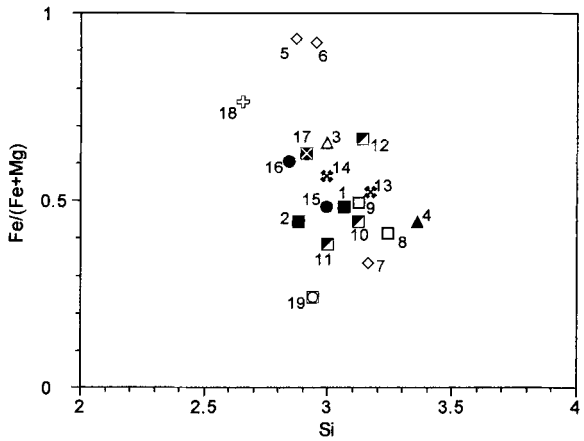

Figure 1. Plot of Fe/(Fe + Mg) ratios vs. Si contents of chlorites. The sample numbers are the same as in the Table 2. Identical symbols correspond to the same well.

$$d_{001} = 14.339 - 0.1155Al^{IV} - 0.0201Fe^{II} \quad [6]$$

into their interplanar spacings d_{001}. These d_{001} values, along with the crystallization temperatures (T °C) and the values of Al^{IV} and Fe required for application of the cited relation, are reported in Table 3. The regression line between T °C and d_{001} obtained by Equation [6] shows a coefficient of correlation (r = −0.702) that is quite similar to that obtained between d^{M}_{001} and T_M (r = 0.77). An even better correlation line, obtained by a least-squares fit, was found between T °C and the values of d_{001} recalculated with an equation of type [5]. In fact, because Equation [1] has been replaced in this new case with Equation [6], Equation [5] becomes:

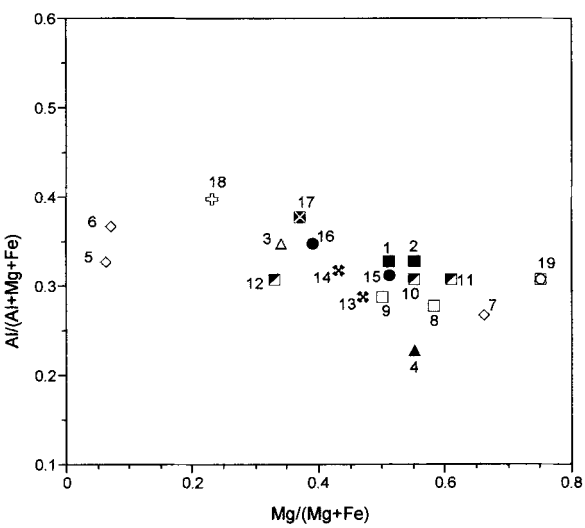

Figure 2. Plot of Al/(Al + Mg + Fe) vs. Mg/(Mg + Fe) ratios of chlorites. The sample numbers are the same as in the Table 2. Identical symbols correspond to the same well.

https://doi.org/10.1346/CCMN.1999.0470106 Published online by Cambridge University Press

Table 2. Measured in-hole (T_M°C) and calculated geothermometric temperatures in °C (T_C; T_{KM}; T_{RX}) for the examined wells. Measured values of (001) and (060) Bragg-lines; values of d^c_{001} and values of Fe(II) calculated with Equations [5] and [2], respectively.

Sample well/Dp. (m)	T_M °C	T_c °C	T_{KM} °C	T_{RX} °C	d^M_{001}	d^M_{060}	d^C_{001}	Fe(II)
1) LA6-670	215	240	253	208	14.249	1.5448	14.173	1.589
2) LA6-1508	300	299	288	274	14.197	1.5470	14.100	1.946
3) LA4-1000	230	263	281	257	14.231	1.5494	14.118	2.332
4) LA3-1450	160	144	187	152	14.310	1.5449	14.236	1.605
5) LA7-550	180	302	327	177	14.208	1.5570		3.567
6) LA7-798	210	276	310	234	14.144	1.5540		3.081
7) LA7-1790	155	208	221	167	14.280	1.5430	14.219	1.297
8) TD1-1588	270	183	210	261	14.194	1.5450	14.114	1.622
9) TD1-2010	250	221	242	246	14.218	1.5460	14.131	1.784
10) TD2-800	200	221	238	200	14.255	1.5445	14.182	1.541
11) TD2-1200	212	260	259	206	14.245	1.5440	14.175	1.459
12) TD2-1500	210	215	250	194	14.189	1.5510		2.600
13) TD3-650	155	109	157	131	14.339	1.5459	14.259	1.768
14) TD3-1440	170	263	274	207	14.260	1.5461	14.174	1.805
15) SL1-1550	160	263	269	174	14.301	1.5470	14.211	1.946
16) SL1-1830	270	311	309	283	14.208	1.5500	14.089	2.432
17) SL2-1330	290	289	296	278	14.199	1.5480	14.095	2.108
18) MV2-1870	285	373	361	291	14.081	1.5560		3.405
19) MV5-1100	325	279	261	305	14.112	1.5405	14.065	0.898
Av. Errors%		24.12	26.93	6.74				

$$d^R_{001} = d_{001} - [0.0107y/(d_{001} - 13.43 + (0.0201y))] \quad [7]$$

The recalculated d^R_{001} are listed in Table 3. In this correlation (T °C vs. d^R_{001}), as in the case of the plot in Figure 4, for 3 samples with an Fe content > 2.6, at temperature (T °C) of 190 (2 samples) and 280 °C, the correction for the Fe/(Fe + Mg) ratio enrichment with Al(IV) was not applied and the d_{001} calculated with Equation [6] were inserted into the correlation. The coefficient of the regression line is r = −0.845 with intercept = 14.286 and slope = −4.92E-04. The formation temperatures recalculated by this regression line (T'_{RX}) are reported in Table 3.

CONCLUSIONS

The good linear correlation reported in Figure 4 shows the consistent results provided by the proposed method. Application of the method to a database on chlorites also gives a good coefficient (r = −0.845) for the regression line correlating T °C with d^R_{001} or d_{001}, for Fe-rich chlorites. The correction for the increase in Al(IV) content of the chlorites with an increase in the Fe/(Fe + Mg) ratio seems to be effective in improving the final results in both experimental data acquisition and database processing, as revealed by several workers (Kranidiotis and MacLean 1987; Jowett 1991). The examined chlorites are authigenic minerals crystallized by water-rock interaction process.

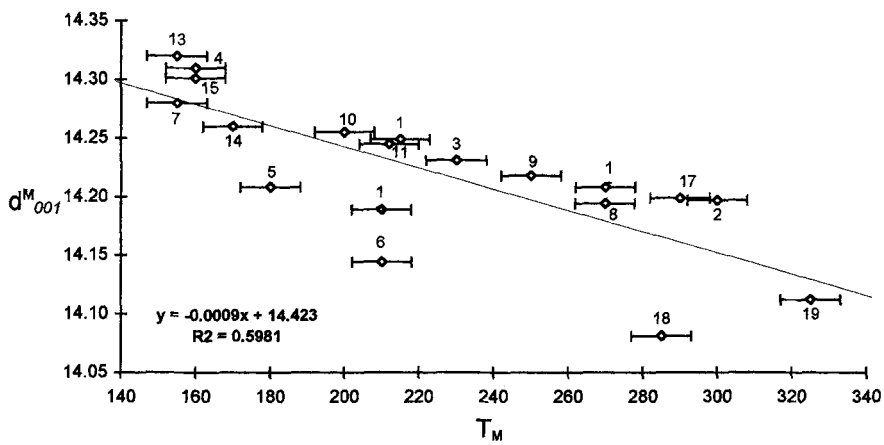

Figure 3. A binary plot of d^M_{001} versus T_M: measured in-hole temperatures in °C for the examined chlorites. Vertical error bars are not reported because they would be hidden by the symbols. Horizontal error bars represent estimated uncertainty in temperature value.

https://doi.org/10.1346/CCMN.1999.0470106 Published online by Cambridge University Press

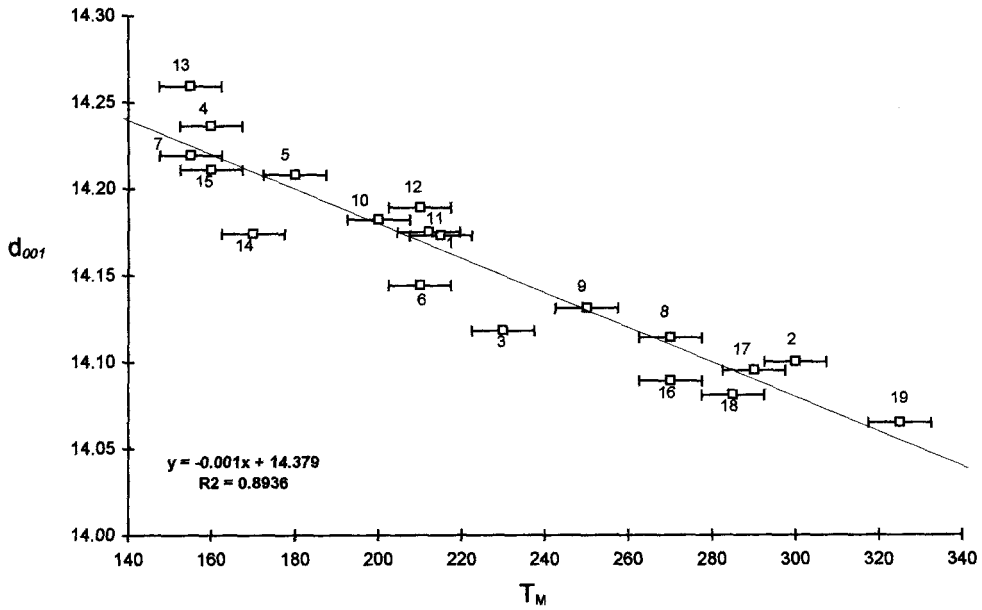

Figure 4. A binary plot of d^{c}_{001} versus T_M, for the samples with Fe(II) content < 2.6; and d^{M}_{001} vs. T_M for the samples with Fe(II) content > 2.6. Vertical error bars are not reported because they would be hidden by the symbols. Horizontal error bars represent estimated uncertainty in temperature value.

Table 3. Data from the literature (Cathelineau 1988) on chlorites from Los Azufres and Salton Sea: values of Al^{IV} and Fe. Values of d_{001} and d^{R}_{001} calculated with Equations [6] and [7], respectively. Estimated temperatures (T °C) at Los Azufres and Salton Sea, and those calculated with the Cathelineau equation (T_c °C) and T'_{RX} (see text), are also reported.

Chlorites						
T °C	Al^{IV}	Fe	d_{001}	d^{R}_{001}	T_c °C	T'_{RX} °C
Los Azufres						
130	0.59	1.08	14.249	14.234	128	148
170	0.71	1.04	14.236	14.222	167	165
180	0.72	1.46	14.226	14.207	170	187
200	0.89	1.14	14.213	14.197	225	201
215	0.91	1.26	14.208	14.190	231	211
235	0.94	1.60	14.198	14.175	241	233
265	0.98	1.68	14.192	14.167	254	245
275	1.03	1.49	14.190	14.168	270	243
280	1.06	1.31	14.190	14.171	279	239
310	1.09	1.75	14.178	14.152	289	266
Salton Sea						
190	1.10	2.93	14.153		292	265
190	1.01	2.83	14.165		263	248
251	0.93	1.95	14.192	14.163	237	250
251	1.11	2.10	14.169	14.137	295	288
264	0.90	2.34	14.188	14.153	228	265
264	1.06	2.03	14.176	14.145	279	276
280	1.12	2.63	14.157		299	259
295	1.09	2.18	14.169	14.135	289	291
295	1.02	2.04	14.180	14.149	266	271
315	1.20	2.55	14.149	14.108	324	330
315	1.11	2.35	14.163	14.126	295	304
322	1.20	2.12	14.158	14.125	324	306
Av. Error%					9.41	8.70

Their presence is always compatible with the observed mineral paragenesis (see geological setting and relevant references) and are present in a wide range of compositions, including the clinochlore, ripidolite, pycnochlorite, diabantite and brunsvigite fields. Therefore, the good overall trend of the regression line for the studied chlorites coming from various geothermal fields suggests that the geothermometer could be applied to chlorites of a wide range of make-ups.

In any case, it should be emphasized that detailed discussion of the use, application range and limitations of such a clay geothermometer is beyond the scope of the present paper (the reader is referred to the chapter on "Use and Misuse of the Geothermometric Relationships" in Cathelineau 1988), which has been limited to the application of the geothermometer method using XRD data. The proposed method, though simpler and less time consuming to implement, provides results that are comparable in accuracy, yet less error-prone than the much more complex techniques currently in use.

REFERENCES

Abbate E, Passerini P, Zan L. 1995. Strike-slip faults in a rift area: A transect in the Afar Triangle, East Africa. Tectonophysics 241:67–97.

Alt JC, Honnorez J, Laverne C, Emmermann R. 1986. Hydrothermal alteration of a 1 Km section through the upper oceanic crust, deep sea drilling project hole 504B: Mineralogy chemistry, and evolution of seawater-basalt interactions. J Geophys Res 91, 10:309–335.

Aquater. 1994a. Tendaho Geothermal Project: Well TD-3: S Lorenzo in Campo (Italy): Government of the Republic of

https://doi.org/10.1346/CCMN.1999.0470106 Published online by Cambridge University Press

Italy Ministry of Foreign Affairs and Government of Ethiopia Ministry of Mines and Energy.

Aquater, 1994b. Tendaho Geothermal Project: Well TD-1, TD-2. S Lorenzo in Campo (Italy): Government of the Republic of Italy Ministry of Foreign Affairs and Government of Ethiopia Ministry of Mines and Energy.

Aspinall WP, Michael MO, Tomblin JF. 1976. Evidence for fluid bodies beneath the Sulphur Springs geothermal region, St. Lucia, West Indies. Geophys Res Lett 3:87–90.

Bailey SW. 1972. Determination of chlorite compositions by X-ray spacings and intensities. Clays Clay Miner 20:381–388.

Baldi P, Bertini G, Ceccarelli A, Dini I, Ridolfi A, Rocchi G. 1995. Geothermal research in the Monteverdi Zone (western border of the Larderello Geothermal Field). Proc World Geothermal Congress; Florence, Italy 2:693–696.

Battaglia S, Gianelli G, Rossi R, Cavarretta G. 1991. The sulphur springs geothermal field, St. Lucia, Lesser Antilles: Hydrothermal mineralogy of wells SL-1 and SL-2. J South Am Earth Sciences 4:1–12.

Bence AE, Albee AL. 1968. Empirical correction factors for the electron microanalysis of silicate and oxides. J Geol 76: 382–403.

Bettison LA, Schiffman P. 1988. Compositional and structural variations of phyllosilicates from the Point Sal ophiolite, California. Am Mineral 73:62–76.

Bettison-Varga LA, MacKinnon IDR. 1989. Comparison of microanalytical techniques used in the characterization of mixed layer chlorite/smectite from the Point Sal ophiolite. Clay Miner Soc 26th Annu Meet.

Bevins RE, Robinson D, Rowbotham G. 1991. Compositional variations in mafic phyllosilicates from regional low-grade metabasites and application of the chlorite geothermometer. J Metamorphic Geol 9:711–721.

Brindley GW. 1961. Kaolin, serpentine and kindred minerals. In: Brown G, editor. The X-ray identification and crystal structures of clay minerals. London: Mineral Soc. p 51–131.

Cathelineau M. 1988. Cation site occupancy in chlorites and illites as a function of temperature. Clay Miner 23:471–485.

Cathelineau M, Nieva D. 1985. A chlorite solid solution geothermometer The Los Azufres (Mexico) geothermal system. Contrib Mineral Petrol 91:235–244.

De Caritat P, Hutcheon I, Walshe JL. 1993. Chlorite geothermometry: A review. Clays Clay Miner 41,2:219–239.

Deer WA, Howie RA, Zussman J. 1962. Rock forming minerals. 3. Sheet silicates. New York: J Wiley. p 270.

Di Paola GM. 1972. The Ethiopian Rift Valley (between 7°00′ and 8°40′ lat. North). Bull Volcanol 36(4):517–559.

Electroconsult ELC. 1986. Exploitation of Langano-Aluto geothermal resources. Feasibility report, Milan, Italy. 87 p.

Foster MD. 1962. Interpretation of the composition and a classification of the chlorites. US Geol Surv Prof Pap 414A:1–33.

Gianelli G, Bertini G. 1993. Natural hydraulic fracturing in the Larderello Geothermal Field: Evidence from Well MV5A. Boll Soc Geol It 112:507–512.

Gianelli G, Teklemariam M. 1993. Water-rock interaction processes in the Aluto-Langano geothermal field (Ethiopia). J Volcan Geoth Res 56:429–445.

Helmold KP, Van de Kamp P. 1984. Diagenetic mineralogy and controls on albitization and laumontite formation in Paleogene arkoses, Santa Ynez mountains, California. In: McDonald D, Surdam R, editors. Clastic digenesis. Am Assoc Petrol Geol. p 239–276.

Hey MH. 1954. A new review of the chlorites. Mineral Mag 30:277–292.

Hochstein MP, Caldwell G, Kifle K. 1983. Minimum age of the Alutogeothermal system. Internal report, Geothermal Institute, Univ of Auckland. 3 p.

Inoue A, Utada M, Nagata H, Watanabe T. 1984. Conversion of trioctahetral smectite to interstratified chlorite/smectite in Pliocene acid pyroclastic sediments of the Ohyn district, Akita Prefecture, Japan. Clay Sci 6:103–116.

Jahren JS, Aagaard P. 1989. Compositional variations in diagenetic chlorites and illites, and relationships with formation-water chemistry. Clay Miner 24:157–170.

Jowett EC. 1991. Fitting iron and magnesium into the hydrothermal chlorite geothermometer. GAC/MAC/SEG Joint Annu Meet Toronto; 27–29 May. Prog with Abstr 16:A62.

Kepezhinskas KB. 1965. Composition of chlorites as determined from their physical properties. Dokl Akad Nauk SSSR, Earth Sci Sect 164:126–129.

Kranidiotis P, MacLean WH. 1987. Systematics of chlorite alteration at the Phelps Dodge massive sulfide deposit, Matagami, Quebec. Econ Geol 82:1898–1911.

Laird J. 1988. Chlorites: Metamorphic petrology. In: Bailey SW, editor. Hydrous phyllosilicates. Rev Mineral 19:405–454.

Lloyd EF. 1977. Geology factors influencing geothermal exploration in Langano region, Ethiopia. N.Z. Geol Surv UN Geothermal Project in Ethiopia. 73 p.

MacDowell SD, Elders WA. 1980. Authigenic layer silicate minerals in borehole Elmore 1, Salton Sea geothermal field, California, USA. Contrib Mineral Petrol 74:293–310.

Mickledust RL, Fiori CE, Heinrich KFS. 1978. A compact procedure for quantitative energy dispersive electron probe X-ray analysis. US Natl Bur Stand Tech Note.

Nemecz E. 1981. Clay minerals, Akademiai Kiado, Budapest, Hungary.

Nieto F. 1997. Chemical composition of metapelitic chlorites: X-ray diffraction and optical property approach. Eur J Mineral 9:829–841.

Rausell-Colom JA, Wiewiora A, Matesanz E. 1991. Relation between composition and d_{001} for chlorite. Am Mineral 76: 1373–1379.

Reynolds RC. 1988. Mixed-layer chlorite minerals. In: Bailey SW, editor. Hydrous phyllosilicates. Rev Mineral 19:601–629.

Roberson HE. 1989. Corrensite in hydrothermally altered oceanic crustal rocks. Clay Miner Soc 26th Annu Meet (abstract). p 59.

Rose AW, Burt DM. 1979. Geochemistry of hydrothermal ore deposits (hydrothermal alteration). New York: J Wiley.

Shau YH, Peacor DR, Essene EJ. 1990. Corrensite and mixed-layer chlorite/corrensite in metabasalt from northern Taiwan: TEM/AEM, EMPA, XRD, and optical studies. Contrib Mineral Petrol 105:123–142.

Schiffman P, Fridleiifsson GO. 1991. The smectite–chlorite transition in drillhole NJ-15, Nesjavellir geothermal field, Iceland: XRD, BSE and electron microprobe investigations. J Metamorphic Geol 9:679–696.

Shirozu H. 1958. X-ray powder patterns and cell dimensions of some chlorites in Japan, with a note on their interference colors. Mineral J (Japan) 2:209–223.

Shirozu H. 1978. Developments in sedimentology (Chlorite minerals), vol. 26. New York: Elsevier. p 243–264.

Steiner A. 1977. The Wairakei geothermal area, North Island, New Zealand: Its subsurface geology and hydrothermal rock alteration. Bull New Zealand Geol Surv 90:136.

Teklemariam M, Battaglia S, Gianelli G, Ruggieri G. 1993. Changes in temperature and salinity in a zone of lateral flow in the Aluto-Langano geothermal field, Ethiopia: Evidence from clay minerals and fluid inclusions. In: Fenoll Hach-Ali, Current research in geology applied to ore deposit. Torres-Ruiz Gervilla, editors. 775–778.

Teklemariam M, Battaglia S, Gianelli G, Ruggieri G. 1996. Hydrothermal alteration in the Aluto-Langano geothermal field, Ethiopia. Geothermics 25(6):679–702.

Von Engelhardt W. 1942. Die Strukturen von Thuringit, Bavalit und Chamosit und ihre Stellung in der Chloritgruppe. Kristallogr 104:142–159.

Westercamp D, Tomblin J. 1980. Le volcanisme rècent et les éruptions historiques dans la partie centrale de l'arc insulaire des Petites Antilles. Bull Bur Rech Geol Min, Ser. 2, 3/4:293–319.

Wohletz K, Heiken G, Ander M, Goff F, Vautaz FD, Wadge G. 1986. The Qualibou caldera, St. Lucia, West Indies. J Volcanol Geotherm Res 27:77–115.

(Received 28 April 1997; accepted 4 August 1998; Ms. 97-040)